International Journal of Modern Manufacturing Technologies
ISSN 2067–3604, Vol. XIV, No. 1 / 2022
https://doi.org/10.54684/ijmmt.2022.14.1.23

INVESTIGATION OF AUTOMATIC BED LEVELLING SYSTEM FOR FUSED DEPOSITION MODELLING 3D PRINTER MACHINE

Dundesh S Chiniwar[1], Harsha Alva[2], Vijay Raghav Varada[3], Mallikarjuna Balichakra[4], Shivashankar Hiremath[1]

[1]Department of Mechatronics, Manipal Institute of Technology, Manipal Academy of Higher Education, Manipal, Karnataka 576104, India
[2]Daimler Truck Innovation Center India Private Limited, Whitefield Palms, Bangalore Karnataka, India
[3]Fracktal Works Private Limited, Peenya, Bangalore Karnataka, India
[4]Department of Mechanical Engineering, Amrita School of Engineering, Coimbatore, Amrita Vishwa Vidyapeetham, India.

Corresponding author: Shivashankar Hiremath, sssnitk@gmail.com

Abstract: The current paper describes a new low-cost sensing system that employs a load cell embedded in the tool carriage assembly of an open hardware fused deposition modelling (FDM) 3D printer. The sensor system automates the process of detecting and compensating for inconsistencies in the flatness of the bed's surface relative to the nozzle. A sensor system prototype was implemented in an FDM 3D printer to determine contact between the bed and the tool's nozzle. The system was then used by a software routine in the machine's microcontroller firmware to automate the bed levelling. Finally, an automated bed leveling system was observed and analyzed its behavior.
The sensor system and the Automatic Bed Levelling (ABL) process are evaluated by observing the bed surface obtained via a load cell bed probe. From the machine controller, the ABL process takes 75 seconds. The bed levelling system uses the load cell probe to automate the manual bed levelling process, saving time. The current work reduces error and improves the efficiency of 3D printer operation. It also reduces the amount of time needed to operate and improves print quality.

Keywords: Automatic bed; 3D printer; Load cell; Bed levelling; Fused deposition modelling

1. INTRODUCTION

Nowadays, 3D printing is used not only for rapid prototyping but also for designing new components and production. In recent years, the world has witnessed phenomenal growth in the 3D process. Currently, 3D technology is used in a variety of industries ranging from medicine to aviation to food [1-4]. 3D printing technology is a developing field with opportunities for innovation in the design of new products/components, software development, interfacing and regulating machines using electronic devices to improve manufacturing efficiency, and many other areas [5, 6]. This technology has also gained popularity in the media, in the public's imagination, and among researchers in various fields. Recently, there has been a surge in interest in this technology, which is constantly being redefined, reimagined, redeveloped, recreated, and customized for a diverse range of products [7, 8].
3D printing stacks multiple layers on top of each other to create a three-dimensional object. The majority of 3D print layers are extremely thin, ranging in thickness from 10 to 200 microns. The print effect across the layer is determined by the nozzle feeder, bed level, material, and other parameters [9-11]. Material modelling, tool design, computing parameters, and process design are the primary challenges for both researchers and the 3D printing industries. For example, in fused deposition modelling (FDM) technology, process parameters such as printer bed surface and flatness, feeder, temperature, motor driver, and nozzle clogging can be identified before the process, which may help to improve the 3D printer as well as a printed product.
According to some surveys, 20% of printer failures are caused by inexperienced users and incorrect printer usage. The main reason for this is that the filament extruder may miss the printing platform; the extruder may stop in the middle of a print due to clogging or slipperiness in the motor driver; the print part may not stick to the bed; the copy peels away from the platform or wraps; inaccurate dimensional of the components; and many more [12-14]. In addition, the height of the initial layer of a 3D print influences bed adherence, surface finish, and overall component print quality [15].
The minimum bed distance between the nozzle and the bed during the extrusion of the initial layer, according to the authors [16], should be about the thickness of one sheet of paper. If the gap is too large, it may cause adhesion issues; if the distance is too small, the filament may not melt from the nozzle [17].

The use of a sensor that is often connected to the hot end assembly to facilitate the bed levelling process is an advanced application in 3D printing. The sensor is positioned around 1mm above the nozzle tip. Before a print, the sensor calculates the distance between the sensor tip and certain bed parts. During the laydown of the initial layer of extruded plastic on the bed, the sensor calculates the height of each point on the bed and adjusts the z offset. The quality of the initial layer of printing impacts the quality of the entire model in 3D printing. The model could most likely fail if the first layer is not printed properly. 3D printer bed levelling is one of the most critical variables for model formation; an uneven print bed might produce unexpected issues with the first layer of 3D printing. As a result, the printed model adheres poorly. If the nozzle is placed too close to the printing bed, it can become clogged. It is extremely difficult to obtain precise data on the bed level with the sensor. In addition, bed levelling accounts for 12 to 26 percent of machine and 3D printed part failures [18, 19]. Addressing automatic bed levelling issues in 3D printing technology is critical for the research community.

The current article focuses on an automated bed levelling system that uses a load cell as a touch probe to implement real-time 3D printer path tracing. The technique is implemented in an open hardware FDM 3D printer using the open-source Marlin microcontroller firmware. The bed adjustment accounts for the inconsistencies in the flatness of the bed during each layer. The proposed technique saves time spent manually calibrating the bed and allows low-skilled users unfamiliar with the bed's manual probing to access the printers.

2. METHODOLOGY

The uneven bed surface may cause manufacturing defects or warping of the layer as it is heated. This can be compensated for by tilting the bed plane while printing and accounting for inconsistencies in real-time. At the start, the bed is probed to detect errors in flatness. The nozzle is moved to several known points on the bed surface, either four or nine. The gap between the bed and the nozzle is calibrated by placing a sheet of bed size paper between them and adjusting the Z-axis (vertical) using the touch screen (Human Machine Interface) until the paper is tightly gripped. The Z-axis position is recorded at each calibration point, and the process is repeated at the next point. This process's output is saved to the operator's memory as a mesh of two-dimensional points on the bed (i.e., x, y) and the corresponding Z position. The compensation for Z offsets at any point (x, y) on the bed is generated during printing using bilinear interpolation on the saved mesh. As a result, the printing plane is more even, which improves bed adhesion and overall print quality. The mesh bed levelling probing process is time-consuming and requires operator intervention. A manual bed levelling operation can produce a levelled bed in a matter of minutes. Thus, automatic bed levelling can save time and manual error while providing an accurate value for all coordinates.

2.1 Bed sensing techniques

For automatic bed levelling, marlin firmware supports a variety of probe configurations. A digital signal reader is used to determine whether the bed is in contact with the nozzle. Other touch probe options are explained here, a commonly used technique.

Microswitch probes are one of the most basic options for touch probes, as illustrated in Figure 1. Because the switch extends below the nozzle, they must be stowed while printing to avoid collisions with the part being printed. The deployment of the probe necessitates the use of additional mechanisms, which complicates the extruder assembly. The disadvantage of using micro switches as probes is that they add mass and have poor repeatability due to moving parts.

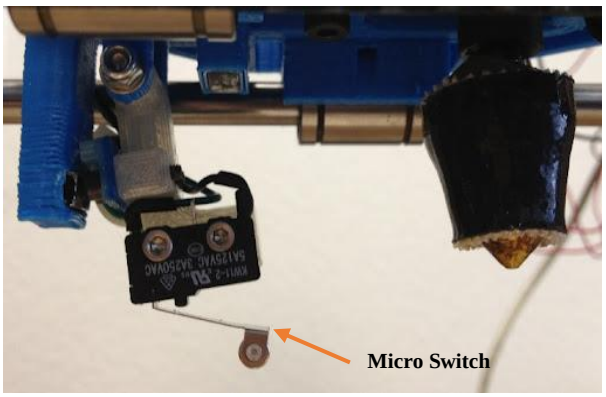

Fig.1 Shows the microswitch probe is used in the automated level technique

Marlin firmware also supports proximity sensors, whether inductive, capacitive, or optical. They are non-contact and detect the bed from a distance of 8 to 12 mm, depending on the sensor used. They are highly accurate and generally repeatable. Figure 2 depicts the inductive proximity sensor used for 3D printer bed levelling. The issue is the proper mounting of the proximity sensor and the additional cost of the 3D machine.

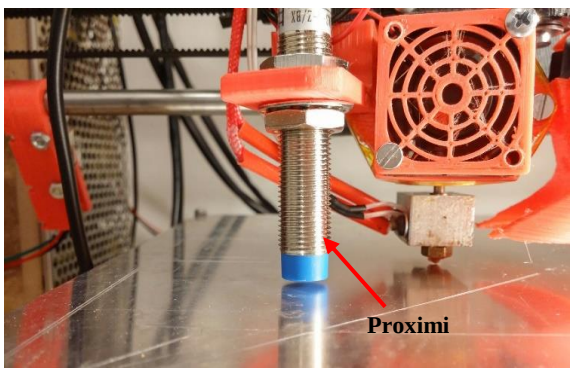

Fig. 2 Inductive proximity sensors for automatic bed levelling

A piezoelectric sensor is another important bed levelling detector sensor found in 3D printers. Piezoelectric touch probes have been used in two configurations: under the bed and at the tool's hot end. A suitable electronic circuit is used to condition the output voltage generated by the member. Three piezoelectric discs are mounted at three points on the Z platform, where the bed is suspended using specially designed mountings in the under-bed configuration, as shown in Figure 3. These have a higher level of support complexity, can detect X and Y movements, and their sensitivity is affected by the temperature of the bed. The nozzle is suspended on a specially designed 3D printed part mounted to the carriage in the hot end probe configuration. When the nozzle comes into contact with the bed, a piezoelectric disc integrated into the 3D printed mount deflects. Allow the filament supply to the nozzle, and a hole must be drilled into the member. Piezoelectric touch probes necessitate complex mounting and calibration to detect bed levels.

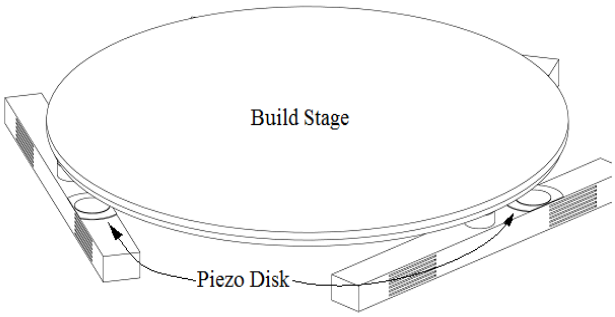

Fig. 3. Piezoelectric touch probes for bed levelling

The sensors mentioned above are complex, require additional mounting, and are separate from the nozzle, necessitating offsets.

As a result, a touch probe for a 3D printer with a bed dimension of 400 mm x 400 mm is being developed. It uses a strain gauge load cell integrated into the carriage assembly (tool mount point) and uses the tool nozzle as a contact surface while probing.

2.2. CAD model for load cell placement

The touch probe is powered by a load cell that is built into the carriage assembly. The computer-aided design (CAD) is used to better comprehend the 3D printer parts shown in Figure 4(a) and (b). It is installed so that one end of the load cell is attached to the carriage plate, which is attached to the linear guide bearing on which the carriage travels. Two mm spacers connect the tool plate, on which the cold end of the tool is mounted, to the carriage plate on one side. The load cell's other end is attached to the opposite side of the tool plate. This configuration enables the tool plate to flex about an axis parallel to the linear guide travel, i.e. the X-axis. Based on the CAD model, the same carriage is built. The carriage assembly is tested and studied for durability after being mounted on the 3D printer machine.

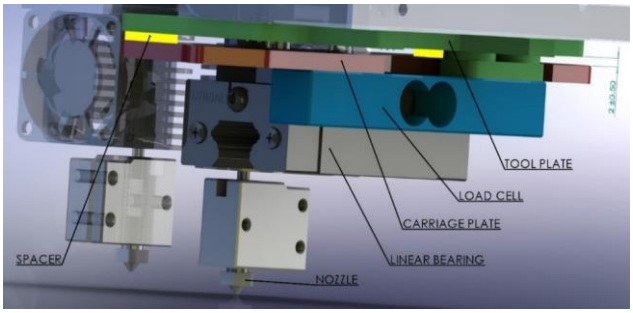

(a)

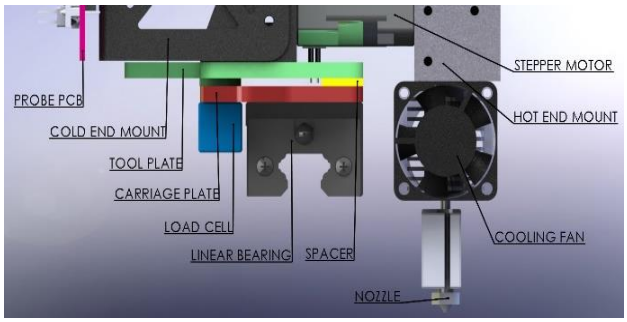

(b)

Fig.4. Shows the CAD model of (a) Front end of carriage assembly (b) Back end of the carriage assembly of the 3D printer machine

2.3 Signal conditioning of the load cell

The load cell used is a TAL220B strain gauge with a load capacity of 5 kg and a rated output of 1mV/V of input at full load. At full load, the output of the used load cell is 5mV for a 5V excitation voltage. The touch probe is equipped with the HX711 load cell amplifier circuit [20]. It operates on a supply voltage range of 2.6-5.5V. It includes a built-in voltage regulator for load cell excitation as well as a 24-bit Analog to Digital converters, a programmable differential amplifier with 32, 64, or 128 selectable input differential gain, and a data output rate of 10Hz or 80Hz. The output is linear, and the differential input signal is scaled to the supply voltage level.

The circuit uses serial interfacing for control and data transfer communication with a microcontroller. The two pins are PD_SCK (Power Down & Serial Clock Input) and DOUT (Serial Data Output). The output data is coded in 2's complement to store negative values and must be decoded with the factor 0x800000 to get the load cell value. The output value is then scaled differential input between no load and full load conditions and must be converted to physical units with suitable methods. The circuit is controlled by specific pin states and needs accurate clock pulses to retrieve the load cell value and set the gain. A microcontroller extracts the data and converts it to a digital signal based on a threshold to detect nozzle contact. The steps to

transmit and detect the signal are shown in the two-pin timing diagram in Figure 5(a). The flowchart is shown in Figure 5(b) explains the steps to access the data from the ADC.

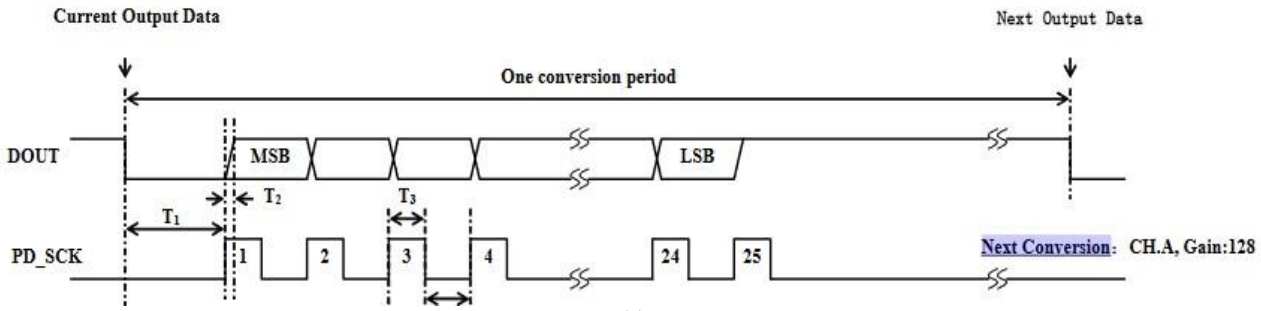

(a)

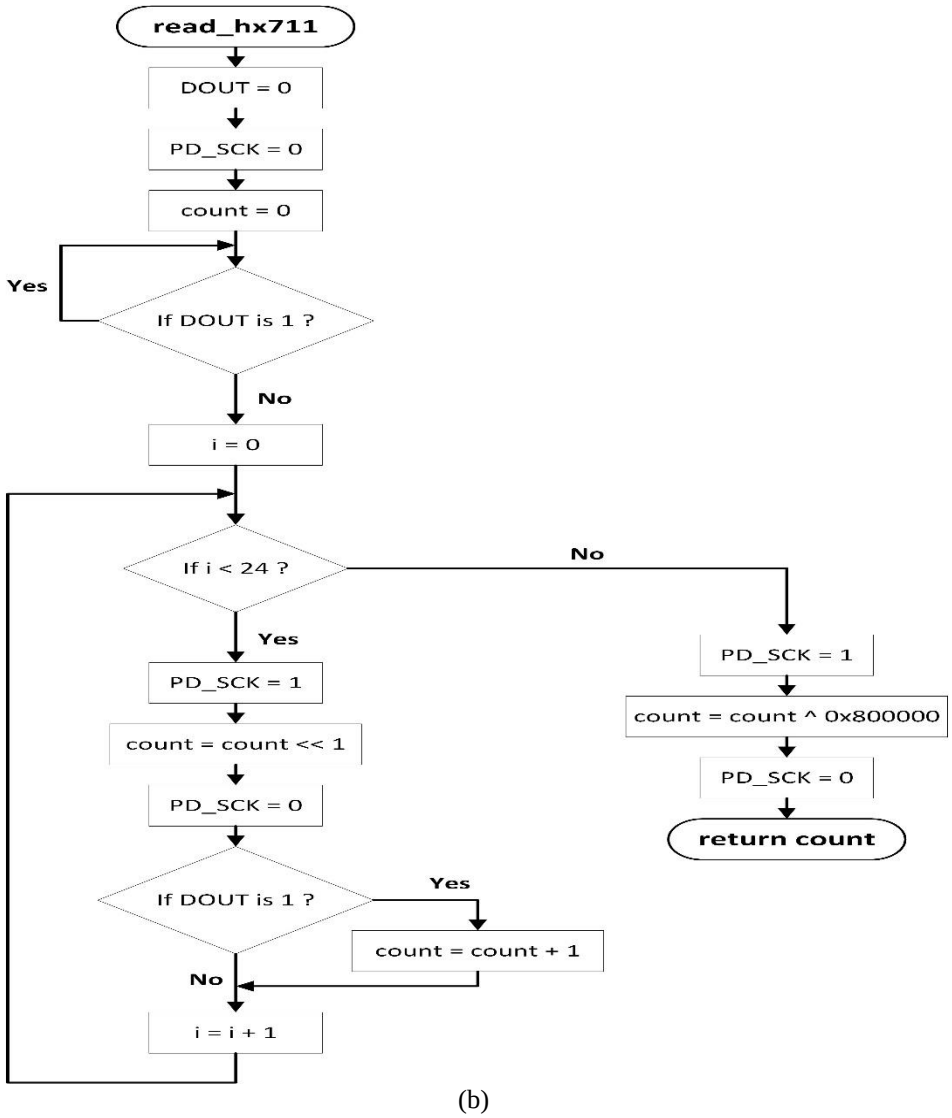

(b)

Fig.5. Shows the (a) Timing diagram of load cell (b) Flowchart of access data from ADC

2.4 Circuit layout for detecting the contact surface

The machine controller anticipates a digital signal from the touch probe to determine whether the bed has contacted the nozzle. After processing the data received from the HX711 IC, an electronic circuit using a microcontroller converts it to a digital signal.

The circuit layout for acquiring data from the load cell, which is mounted on the carriage and is installed on a two-layer PCB, is shown in Figure 6. The load cell amplifier (HX711 IC) enhances the load cell signal and converts it from analog to digital. The filtered signal is supplied to the ADC by the power condition circuit. The microcontroller development board, which is based on the Atmel ATmega328p 8-bit microcontroller, is used to provide clock pulses to read the HX711 IC and output a digital signal to

indicate contact. When the nozzle comes into contact with the bed, an LED highlights to alert the user. Furthermore, the load cell is placed close to the amplifier to reduce noise and errors. In an edge-sensitive interrupt, a firmware is developed to detect the contact surface and read the direction of the bed movement from the machine controller. The level of the Z-axis direction changes, and the interrupt service routine (ISR) is invoked. When the bed is moving towards the nozzle, probing is detected. When probing is active, the HX711 IC reads the amplified load cell readings from the IC and converts them to physical units in grams. When the converted reading crosses a threshold, send the digital signal to the machine controller. Any output debugs data sent to the serial interface when inactive probing and deactivates the microcontroller and the HX711 IC.

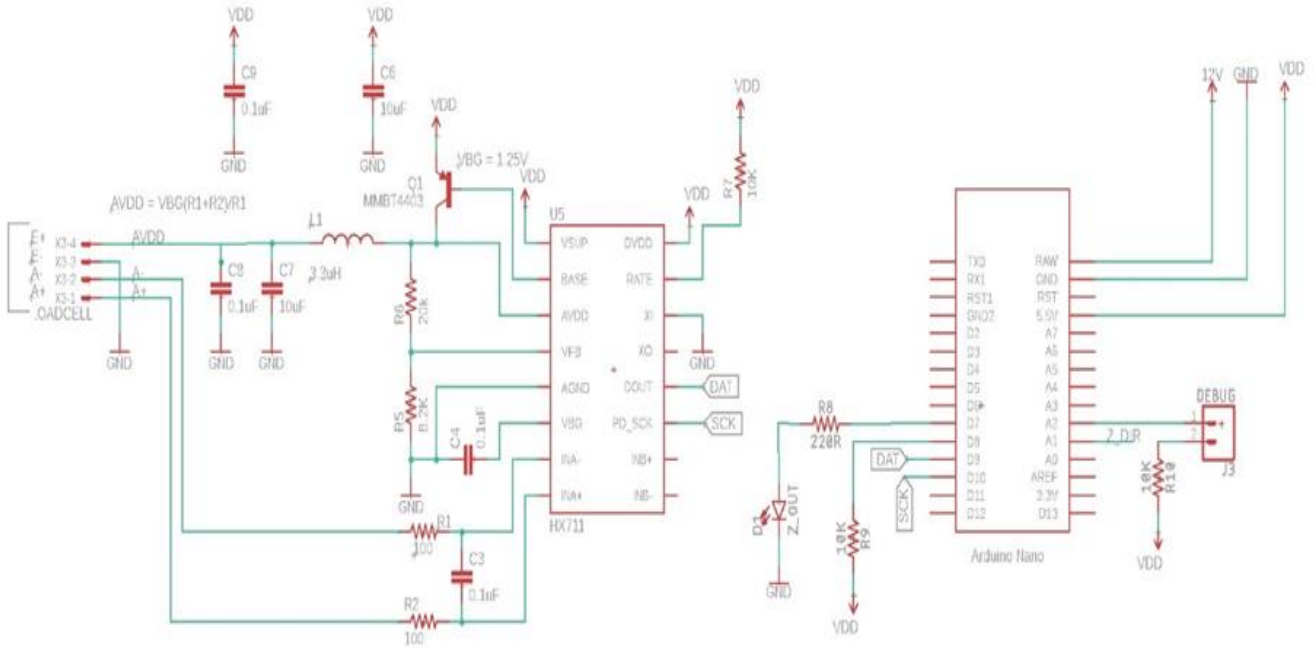

Fig.6. Shows the circuit layout design for detecting the contact surface

The same firmware is developed for the microcontroller to perform and detect the surface related to probing. The firmware created for the microcontroller is based on the Arduino library (HX711 ADC) to reduce the implementation time. A calibration factor of 700 aids in dividing the IC reading into a smaller value. It can be stored in a 1-byte floating-point variable with a range of -256 to +255. The microcontroller's and firmware's operations can be divided into two states. First, the microcontroller invokes the setup routine, which initializes GPIO, variables, and objects. The microcontroller then enters the endless loop stage, in which it continuously monitors the load cell readings, compares them to a threshold, and then updates the triggered signal. The flow chart for detecting the bed's surface is shown in Figure 7.

Each step of the flow chart is explained in the setup phase and loop phase. Reading the load cell ADC output, the setup phase initializes the "ADC Loadcell" object based on the HX711 ADC library class. The touch detection trigger is sent to the machine controller via GPIO after the bed direction state has been read. The current bed direction is then set in the global variable "old bed dir." This variable is used to detect changes in bed direction between endless loop iterations.

In the case of Loop Phase "ADC Loadcell," to prepare for a new reading and read the local variable "current bed dir." with the current bed direction state. If the value of "current bed dir." indicates that the bed is moving away from the nozzle, set the trigger to LOW and repeat the endless loop. Furthermore, if the bed is moving towards the nozzle when it was previously moving away, the load cell value is reweighed through the "ADC Loadcell," the trigger is set to LOW, and the endless loop is repeated. Finally, the load cell's amplified value is read using the "ADC Load Cell" object. If the load cell reading is greater than a threshold factor of 20 to the calibration value, corresponding to an actual reading of 14,000, the trigger output is set HIGH. Otherwise, it is set to a low value. The loop then continues indefinitely.

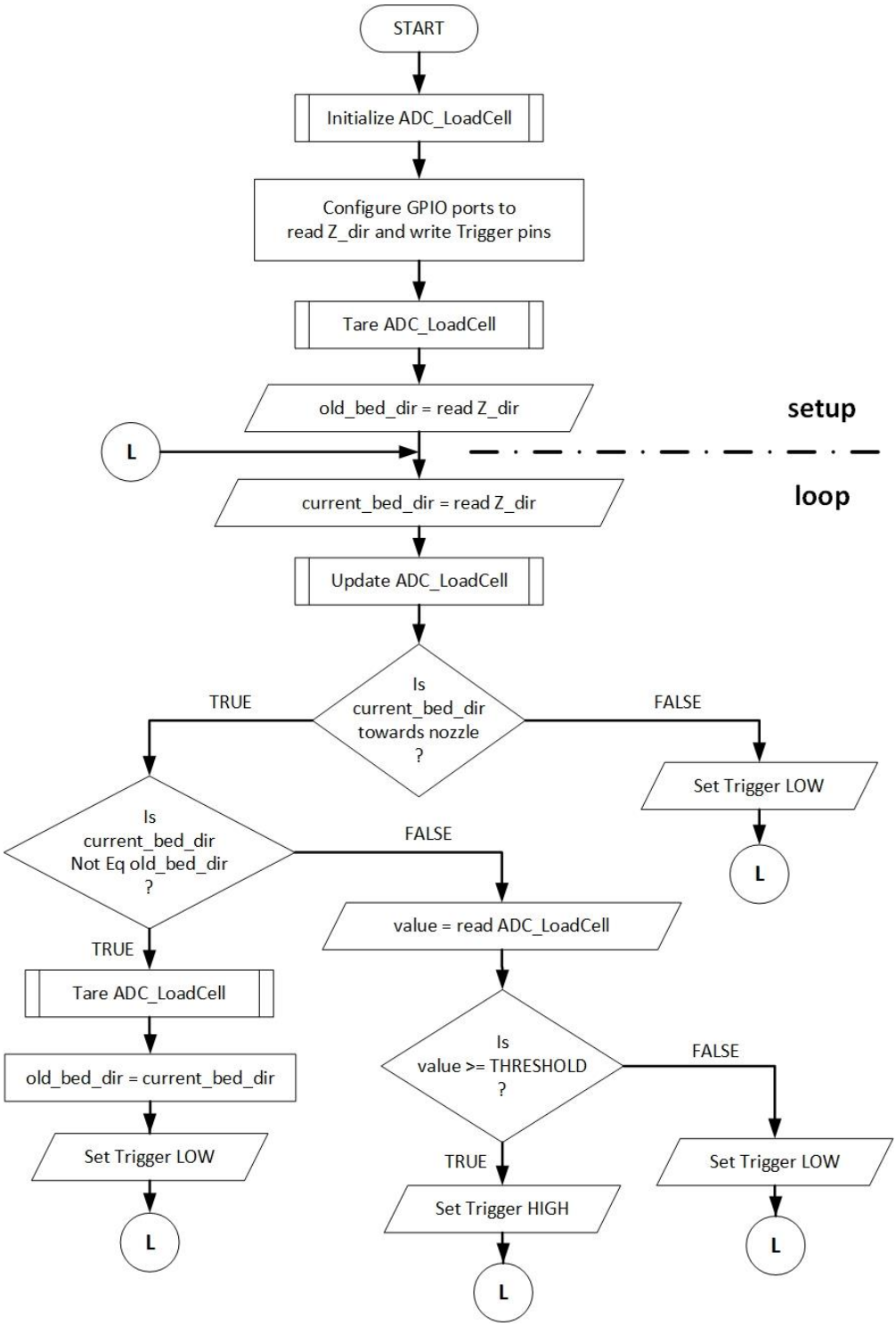

Fig.7. Shows the flow chart for detecting the surface of the bed

2.5 Development of firmware for automatic bed level probe

The ABL probing process is written in C++ and integrated into the custom Marlin firmware. A simple way of understanding the ABL probing method is shown in Fig.8 using the flowchart. The ABL settings are read from memory (EEPROM), and initialized variables are required. Constants such as probe point locations and speeds are calculated based on saved settings. Homing is performed if the tool and bed positions are unknown. The bed is moved 3 mm along the Z-axis, i.e., Z+3. End stops ISR is activated to detect contact between the bed and the nozzle. The nozzle moves directly above the first probing point in the X and Y axes. At a speed of 120 mm/s, the bed is moved to a -2 mm absolute position on the Z-axis i.e., Z-2.

The probe microcontroller reads the load cell readings and sends the contact confirmation signal to the machine controller when the nozzle strikes the bed. The bed motion is halted, and the Z-axis position, z1, is recorded. Suppose the nozzle does not register a hit until -2 mm in the Z position. In that case, an error is generated, and the

machine controller enters a kill state to protect the hardware components from structural damage. The bed is moved 1 mm away from its current position in preparation for the slow pass on a hit. The bed is moved to Z-2 at a speed of 8 mm/s for the second pass. The current Z-axis position z2 is noted upon contact with the nozzle. Because of the forces involved, the variation in speed between passes results in different contact positions. As a result, a weighted Z-axis error value is calculated using equation (1) to account for the varying readings caused by speed, and the result is saved.

$$z = \frac{(z2*3)+(z1*2)}{5} \quad (1)$$

The bed is moved 3 mm away from the nozzle, and the nozzle is moved to a position above the next probing point on the bed. The procedure is repeated for each probing point. The bed topology report is output to the serial interface and is viewable in the host software.

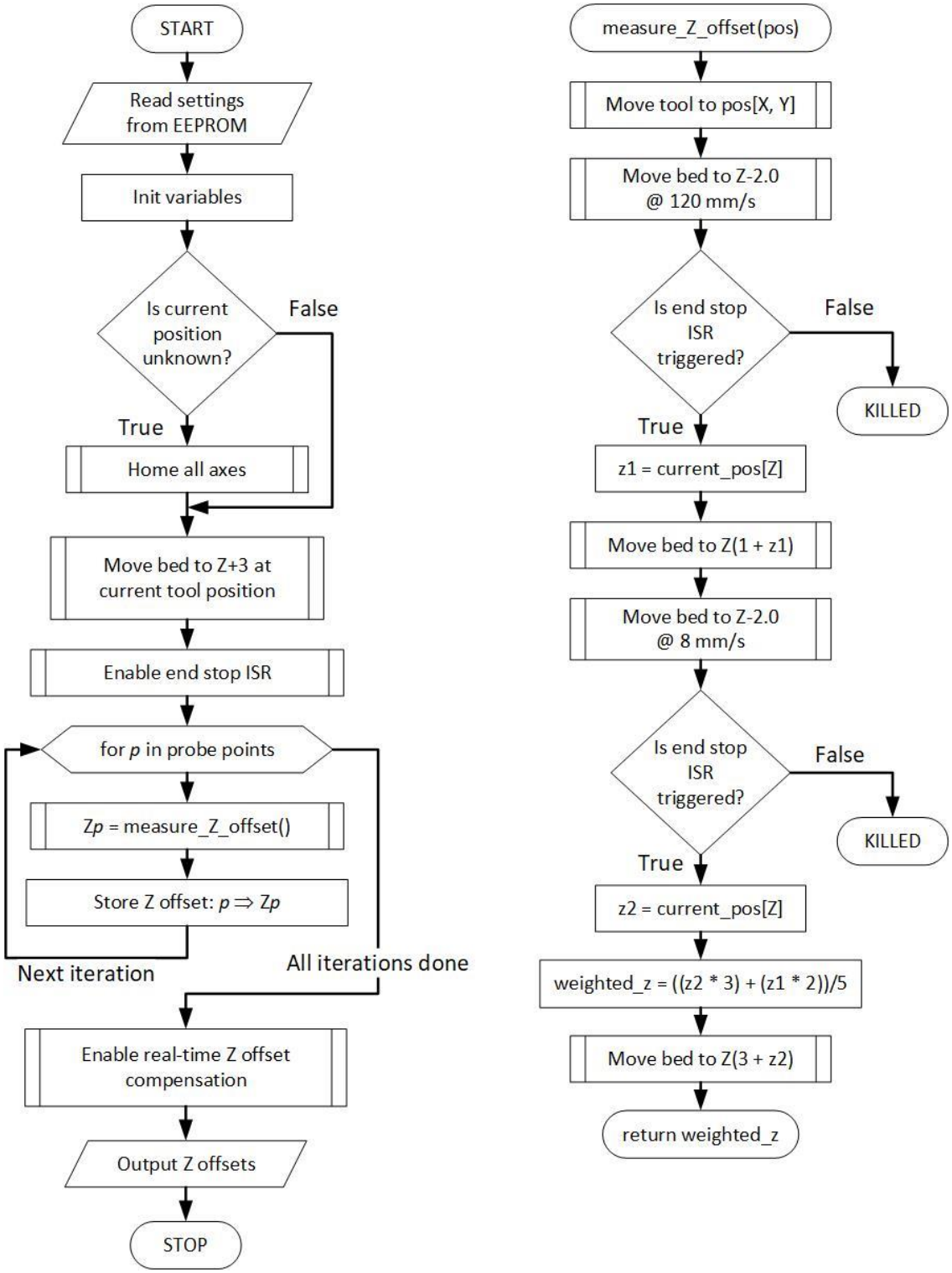

Fig. 8. Shows the flowchart of the integration of firmware and automatic bed levelling probe

3. RESULTS AND DISCUSSIONS

The bed probe sensor system is integrated into the 3D printing machine and controller firmware to automate bed surface levelling. The procedures used to obtain the results, as well as their significance, are discussed further below.

Initially, the printer is calibrated, and the calibration factor is determined using developed firmware and the load cell reading. The code is compiled in the Arduino IDE, flashed to the microcontroller, and the 3D printer machine is tested. The firmware is validated by adjusting the bed level and nozzle with the knob. If the knob is turned loose, the bed will come into contact with the nozzle, as indicated by the LED turning on. The knob is tightened to move the bed away from the nozzle, and an LED light turns off to indicate this. Figure 9 depicts the time required to verify this process. The threshold is set at 20, and the controller takes 25 seconds to cross the bed level and verify the firmware.

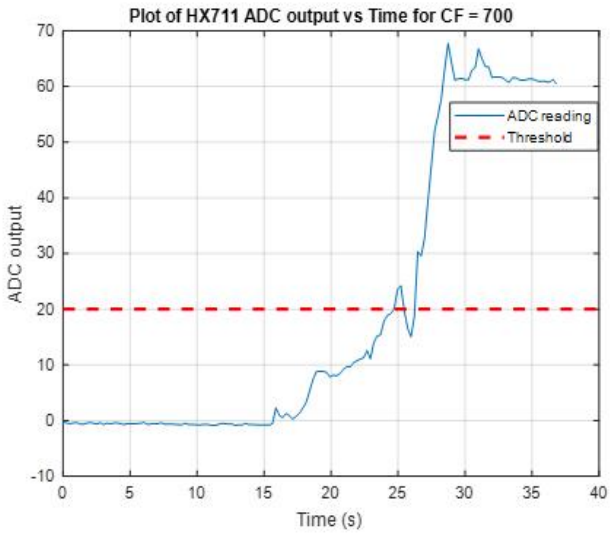

Fig. 9. Shows the verification of the firmware from the ADC output

The firmware includes support for automatic bed level configuration. The firmware enables the bed level to be adjusted to suit the 3D printer machine. Grid size, probe type, number of probe passes, probing area, and offset are some of the most important bed levelling parameters to configure. The working point detected with the touch probe during ABL is shown in Figure 10. The bed size is 400x400mm^2, and the probe size is larger than the printable area. The home position is tested using the nine-point ABL, and readings are taken at each point of the bed. The time required for automatic bed levelling is 75 seconds from start to finish.

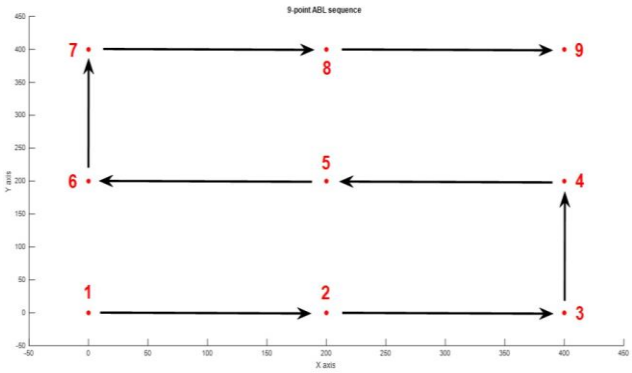

Fig.10. Shows the automatic bed level probe on the flat surface of the bed

The Z offset reading was observed as a result of variations in the bed surface output by the 3D printer machine. The offset is caused by the difference in the flatness of the bed surface. The offset results of the ABL probing process are shown in Table 1. Two passes were used to record the nine-point offset on the flat surface of the bed. A maximum offset of 1.29 mm was noticed at position (400,200), which can be adjusted with proper alignment.

Table 1. Z-offset output of ABL probing process

Point	Location on the bed (mm)		Z-offset readings (mm)		Weighted Z-offset (mm)
	X	Y	First pass, z1	Second pass, z2	
1	0	0	0.11	0.32	0.236
2	200	0	0.35	0.55	0.47
3	400	0	0.15	0.36	0.276
4	400	200	1.14	1.4	1.296
5	200	200	0.4	0.61	0.526
6	0	200	0.15	0.45	0.33
7	0	400	-0.43	-0.22	-0.304
8	200	400	-0.07	-0.28	-0.196
9	400	400	1.52	0.65	0.998

The load cell is the primary unit responsible for sending bed levelling data to the controller. The load cell reading is obtained from the serial monitor and plotted using commercially available software, as illustrated in Figure 11. The spike in the plot represents the bed's contact with the nozzle. Furthermore, the rise and fall of the signal seen above the threshold line are caused by the inertia of the moving bed, which does not stop immediately when the trigger signal is sent to the machine controller.

The load cell is the main unit to send the bed levelling data to the controller. The load cell reading is collected from the serial monitor and plotted using commercially available software, shown in Figure 11.The spike in the plot indicates the contact of the bed with the nozzle. Also, the rise and fall of the signal seen above the threshold line are due to the

inertia of the moving bed, which does not stop instantaneously when the trigger signal is sent to the machine controller. Figure 11(a) collects the nine points from the ADC tare data's two passes, which always lags behind the ADC output signal. The reasons could be due to less time required to transmit data through ADC and a fade in the faster data processing method. The first point signal from the ADC output is shown in Figure 11(b) when the 5th-sec bed touches the nozzle. The time at the fast and slow probing passes is 120mm/s and 8mm/s, respectively, which does not affect the machine's bed levelling.

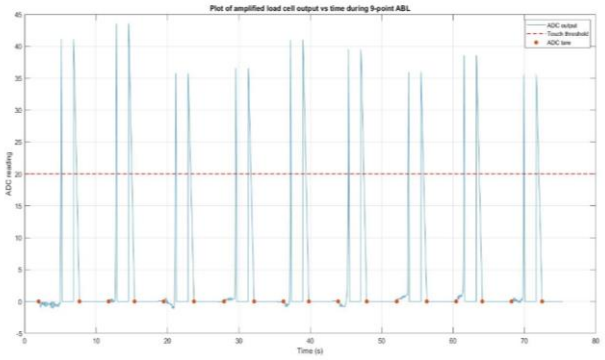

(a)

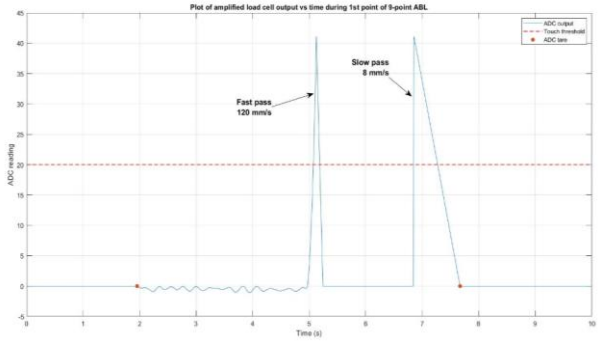

(b)

Fig.11. Shows the (a) Load cell output during the ABL processing (b) 1st point of the ABL signal

Figure 12 depicts the surface plot of the automatic bed level. The amount of variation that occurred during bed levelling is mentioned in the zero planes. The wrap of the bed in the Z-axis demonstrates the inconsistency of the different probe points and is therefore inappropriate. Without user intervention, the ABL system enabled the printer to measure deviations in the flatness of the bed's surface. Variations between -0.304 mm and +1.296 mm from the zero position (Z0) of the bed (Z) axis were observed at various X and Y points. The mean deviation from the Z0 position, around which the real-time path planning compensation is calculated, was +0.8 mm. In comparison to a bed with 200 mm dimensions, measuring the surface of a 400 mm bed took 75 seconds.

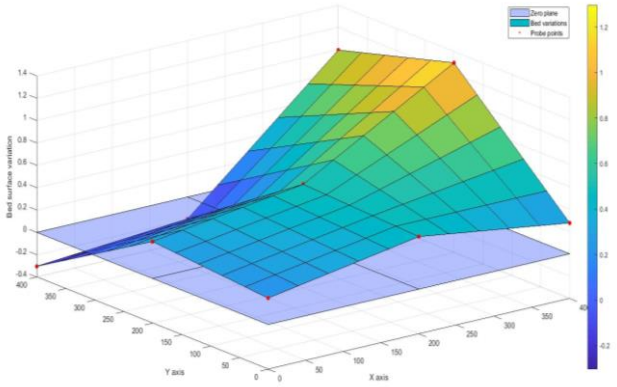

Fig.12. Shows the bed surface observed during the nine-point ABL

4. CONCLUSIONS

A new concept for automated bed levelling has been developed, utilizing a load cell as a touch probe. The system has been integrated and tested in an open hardware FDM 3D printer. The system was discovered to reduce the amount of downtime required to calibrate the machine as well as the errors introduced into the process by a visual feedback-controlled human interaction. Furthermore, it was revealed that it made the machine more approachable to low-skilled users unfamiliar with the manual probing process. The findings of the operations assess the sensor system and the automated bed levelling process. The visualizations of the bed surface were obtained from an automatic bed levelling through load cell data. The ABL process took 75 seconds, as measured by the machine controller's output. Thus, the ABL process, which employs the load cell as a bed probe, is straightforward automation of the manual bed levelling process.

There is a lot of scope for advancement and integration in 3D printer machines. By adding the amplifier IC to the machine controller board and integrating the load cell output comparator firmware functionality into the machine controller firmware, the probe circuit and microcontroller can be eliminated. Another line of investigation into the feasibility of integrating the probe into existing, operational 3D printers can be opened.

5. REFERENCE

1. C. Lee Ventola, (2014), *Medical applications for 3D printing: Current and projected uses*" P T, **39**(10), pp. 704–711.

2. M. Kalender, S. E. Kilic, S. Ersoy, Y. Bozkurt, and S. Salman, (2019), *Additive manufacturing and 3D printer technology in aerospace industry*, Proc. 9th Int. Conf. Recent Adv. Sp. Technol. RAST 2019, pp. 689–695, doi: 10.1109/RAST.2019.8767881.

3. J. Sun, W. Zhou, D. Huang, J. Y. H. Fuh, and G. S. Hong, (2015), *An Overview of 3D Printing Technologies for Food Fabrication*, Food Bioprocess Technol., **8**(8), pp. 1605–1615, doi: 10.1007/s11947-015-1528-6.
4. N. Shahrubudin, T. C. Lee, and R. Ramlan, (2019), *An overview on 3D printing technology: Technological, materials, and applications*, Procedia Manuf., **35**, pp. 1286–1296, doi: 10.1016/j.promfg.2019.06.089.
5. M. Jiménez, L. Romero, I. A. Domínguez, M. D. M. Espinosa, and M. Domínguez, (2019), *Additive Manufacturing Technologies: An Overview about 3D Printing Methods and Future Prospects*, Complexity, vol. 2019, , doi: 10.1155/2019/9656938.
6. G. Putame et al., (2019), *Application of 3D Printing Technology for Design and Manufacturing of Customized Components for a Mechanical Stretching Bioreactor*, J. Healthc. Eng., vol. 2019, doi: 10.1155/2019/3957931.
7. W. Gao et al., (2015), *The status, challenges, and future of additive manufacturing in engineering*, CAD Comput. Aided Des., **69**, pp. 65–89, doi: 10.1016/j.cad.2015.04.001.
8. J. E. Regis, A. Renteria, S. E. Hall, S. Hassan, C. Marquez, and Y. Lin, (2021), *Soft Functional Materials*.
9. K. Brans, (2013), *3D printing, a maturing technology*, IFAC, **46**(7).
10.Y. Tlegenov, W. F. Lu, and G. S. Hong, 2019, *A dynamic model for current-based nozzle condition monitoring in fused deposition modelling*, Prog. Addit. Manuf., **4**(3), pp. 211–223, doi: 10.1007/s40964-019-00089-3.
11.A. Dey and N. Yodo, (2019), *A systematic survey of FDM process parameter optimization and their influence on part characteristics*, J. Manuf. Mater. Process., **3**(3), doi: 10.3390/jmmp3030064.
12.B. T. Wittbrodt et al., (2013), *Life-cycle economic analysis of distributed manufacturing with open-source 3-D printers*, Mechatronics, 23(6), pp. 713–726, doi: 10.1016/j.mechatronics.2013.06.002.
13.S. Nuchitprasitchai, M. Roggemann, and J. M. Pearce, (2017), *Factors effecting real-time optical monitoring of fused filament 3D printing*, Prog. Addit. Manuf., 2(3), pp. 133–149, doi: 10.1007/s40964-017-0027-x.
14.F. Lederle, F. Meyer, G. P. Brunotte, C. Kaldun, and E. G. Hübner, (2016), *Improved mechanical properties of 3D-printed parts by fused deposition modeling processed under the exclusion of oxygen*, Prog. Addit. Manuf., 1(1–2), pp. 3–7, doi: 10.1007/s40964-016-0010-y.
15.N. Volpato, J. A. Foggiatto, and D. C. Schwarz, (2014), *The influence of support base on FDM accuracy in Z*, Rapid Prototyp. J., 20(3), pp. 182–191, doi: 10.1108/RPJ-12-2012-0116.
16.J. Steuben, D. L. Van Bossuyt, and C. Turner, (2015), *Design for fused filament fabrication additive manufacturing*, Proc. ASME Des. Eng. Tech. Conf., **4**, September, doi: 10.1115/DETC2015-46355.
17.C. T. Hsieh, (2016), *Development of an integrated system of 3D printer and laser carving*, Proc. Tech. Pap. - Int. Microsystems, Packag. Assem. Circuits Technol. Conf. IMPACT, 84, pp. 420–423, doi: 10.1109/IMPACT.2016.7800062.
18.Arief RK, Adesta EY, Hilmy I. (2019), *Hardware Improvement of FDM 3D Printer: Issue of Bed Leveling Failures*, Int. J. Technol. Explore. Eng., 8(4).
19. Heras, Enrique Soriano, Fernando Blaya Haro, José María de Agustín del Burgo, and Manuel Enrique Islán Marcos, (2017), *Plate auto-level system for fused deposition modelling (FDM) 3D printers*, Rapid Prototyping Journal, 23(2), pp. 401-413, doi: 10.1108/RPJ-06-2015-0065.
20. Al-Mutlaq, Sarah (2017), *Getting started with load cells*, Conteúdo Online, SparkFun Electron., p. 6, [Online] 2016.

6. ACKNOWLEDGMENT

The authors would like to express their gratitude to Fracktal Works Private Limited, Peenya, Bangalore, Karnataka, India, for all prototype testing.

Received: January 11, 2022 / Accepted: June 15, 2022 / Paper available online: June 20, 2022 © International Journal of Modern Manufacturing Technologies